# CYCLIC FATIGUE BEHAVIOR OF WOVEN HEMP/EPOXY COMPOSITE: DAMAGE ANALYSIS

D. S. de Vasconcellos[1*], F. Touchard[1], L. Chocinski-Arnault[1]

[1]*Institut Pprime, CNRS – ISAE-ENSMA – Université de Poitiers, BP 40109, 86961 Futuroscope Chasseneuil Cedex, France*

**davi.vasconcellos@ensma.fr*

**Keywords:** fatigue, natural fiber, woven composite damage, acoustic emission

## Abstract

*This paper provides results from the characterization of cyclic fatigue behavior of a woven hemp/epoxy composite, constituted by seven layers of hemp fabric and an epoxy matrix. Two types of fabric orientation are tested: $[0°/90°]_7$ and $[\pm 45°]_7$. The cyclic fatigue tests are performed with a frequency of 1 Hz, a stress ratio of 1% (R=0.01) and with different levels of maximum loading. The Acoustic Emission (AE) technique has been applied to measure spatial and temporal positions of cracks and failures during fatigue life, in order to track the damage process. Those results where completed with X-ray microtomography observations and infrared (IR) measurements.*

## 1 Introduction

The worldwide emphasis on environmental awareness triggers scientific researches on the development of recyclable and sustainable composite materials. Recent studies have pointed out hemp fiber composites as a promising option for applications that are currently attended by glass fibers composites and other materials with similar mechanical properties. Furthermore, it is an environmentally sustainable alternative.
Between many works on several types of natural fiber composites, Bonnafous [1] characterized the mechanical properties and damage mechanisms of a woven hemp-fiber/epoxy composite under quasi-static tensile loading. To go further in this eco-composite knowledge, it is necessary to characterize its fatigue behavior. There are few works about cyclic fatigue of natural fiber composites, and most of them are recent. For example, Liang [2] studied the fatigue behavior of flax/epoxy composites and Towo [3] was interested in fatigue behavior of sisal fiber composites. More specifically, about hemp/epoxy composite, Yuanjian [4] studied the fatigue behavior of a hemp mat/epoxy composite.
In this paper, the cyclic tensile-tensile fatigue behavior of a seven layers woven hemp/epoxy composite is characterized. Damage mechanisms are analyzed by using several types of measurements: mechanical parameters, acoustic emission, X-ray microtomography and thermal field by infrared camera.

## 2 Materials and testing methods

### *2.1 Tested specimens*

The studied material is a composite made of 7 plies of balanced 2x2 hemp fabric impregnated with epoxy resin. The hemp fabric is produced by Lin et L'Autre, France, and the epoxy resin is the EPOLAM 2020 from Axson Technologies.

The composite plates are manufactured at the enterprise Valagro by an injection molding process and their fiber volume fraction is 38 ± 5%. The plates are cut at Institut Pprime in two different orientations related to the tensile axis (0°/90° and ±45°). These specimens will be referred as $[0°/90°]_7$ and $[\pm45°]_7$ respectively. The specimens are parallelipipedic and their dimensions are 150x20x3 $mm^3$ (Figure 1), in which the grips take 30 mm of each edge. The specimens were polished to remove mechanical damage caused by the cutting and polishing papers were used in the grips to improve the clamping.

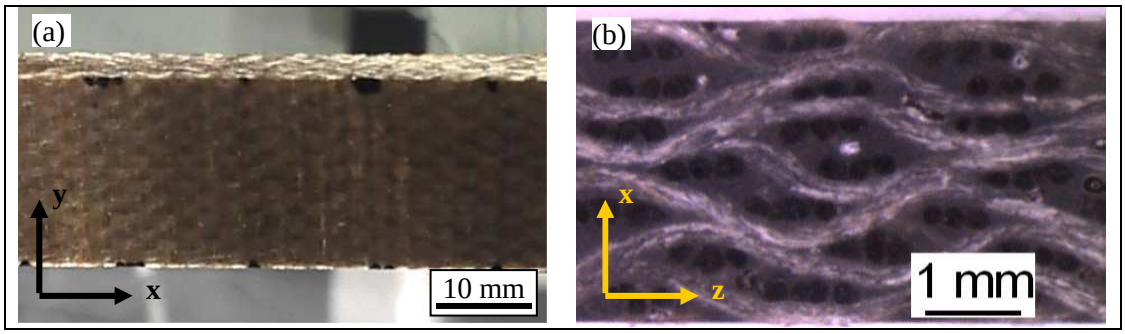


**Figure 1.** Hemp/epoxy $[0°/90°]_7$ specimen: (a) front side, (b) lateral side.

### *2.2 Testing methods*

The fatigue tests were performed with a frequency of 1 Hz, in tensile loading exclusively, and with a ratio between minimum and maximum stress (R) of 0.01 to approach the zero of loading without entering in compression. For each type of woven orientation, three levels of maximum stress were applied and each test was repeated three times. Those levels are:

- for the laminate $[0°/90°]_7$: 40%, 60% and 80% of the quasi-static tensile failure stress (at 0.05 mm/min). That corresponds to three equidistant points on the tensile curve (Figure 2);

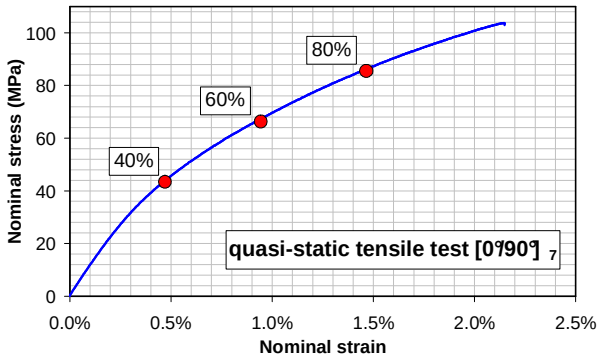


**Figure 2.** Quasi-static tensile stress-strain curve for the $[0°/90°]_7$ hemp/epoxy laminate, with points representing the three levels of loading for the fatigue tests.

- for the laminate $[\pm45°]_7$: 60%, 75%, 90% of quasi-static tensile failure stress (at 0.05 mm/min). That corresponds to points in each of the three regions of the tensile curve: linear zone, transition zone and "plastic" zone (Figure 3).

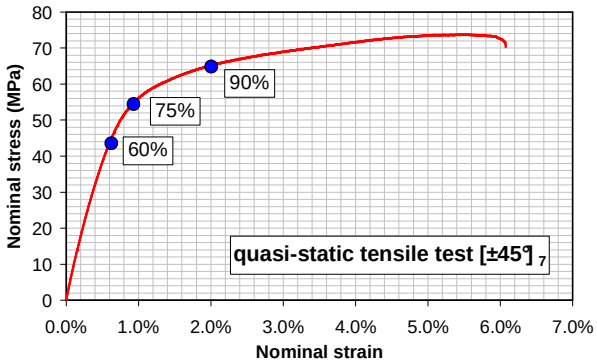


**Figure 3.** Quasi-static tensile stress-strain curve for the $[\pm 45°]_7$ hemp/epoxy laminate, with points representing the three levels of loading for the fatigue tests.

*2.2.1 Acoustic Emission*

Some of the tests were instrumented with acoustic emission (AE) measurement, using the AE system from Physical Acoustics SA. The captors are Micro80 type, with a ceramic face and a diameter of 10 mm. Two captors were placed at the gauge extremities, with a distance of 80 mm between their centers (Figure 4). Acquisition parameters and events definition were taken from Bonnafous work on the same composite [1].

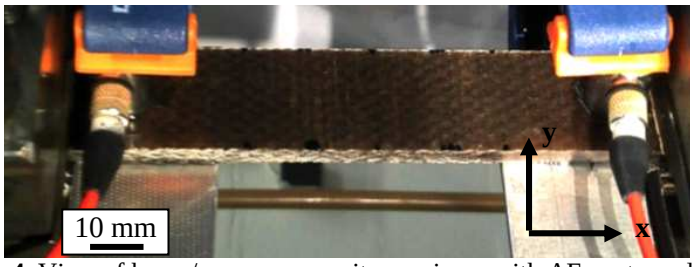


**Figure 4.** View of hemp/epoxy composite specimen with AE captors placed on it.

*2.2.2 Infrared*

An infrared camera from Cedip Infrared Systems with detector resolution of 320x256 pixels and sensibility of 0.1°C was used to measure the temperature evolution at the front side of some specimens during the fatigue tests.

*2.2.3 X-ray microtomography*

At least one damaged sample of each type of specimen and each level of fatigue stress were observed in an X-ray tomograph at the Jean Lamour Institute at Ecole des Mines de Nancy, France. A 20x20 $mm^2$ zone near the rupture was observed with a resolution of 14.8 µm/pixel.

## 3 Results and discussion

*3.1 Fatigue behavior*

The S-N fatigue lifetime curves of the studied material are presented in figure 5, where figure 5.a corresponds to the $[0°/90°]_7$ laminates and figure 5.b to the $[\pm 45°]_7$ ones. In each graph, experimental points and S-N curve determined by the Wöhler model (eq. 1) are plotted. The points with arrows in figure 5.a correspond to the specimens that were not yet broken at one million of cycles.

$$Lg(N_f) = A - B\sigma_{\text{fatigue\_max}} \quad (1)$$

where $N_f$ is the number of cycles at rupture, A and B are material parameters and $\sigma_{fatigue\_max}$ is the applied maximum stress.

In figure 5, it can be seen that there is a significant dispersion in fatigue lifetime results of hemp/epoxy composites, especially for $[0°/90°]_7$ laminates. It is probably due to the natural dispersion of the mechanical properties of hemp fibers, which are directly loaded in tension in $[0°/90°]_7$ laminates. Nevertheless, results show that $[\pm45°]_7$ laminates exhibit higher fatigue lifetime than $[0°/90°]_7$ laminates for a given stress level. And for the two orientations, the Wöhler model is quite in good accordance with experimental points.

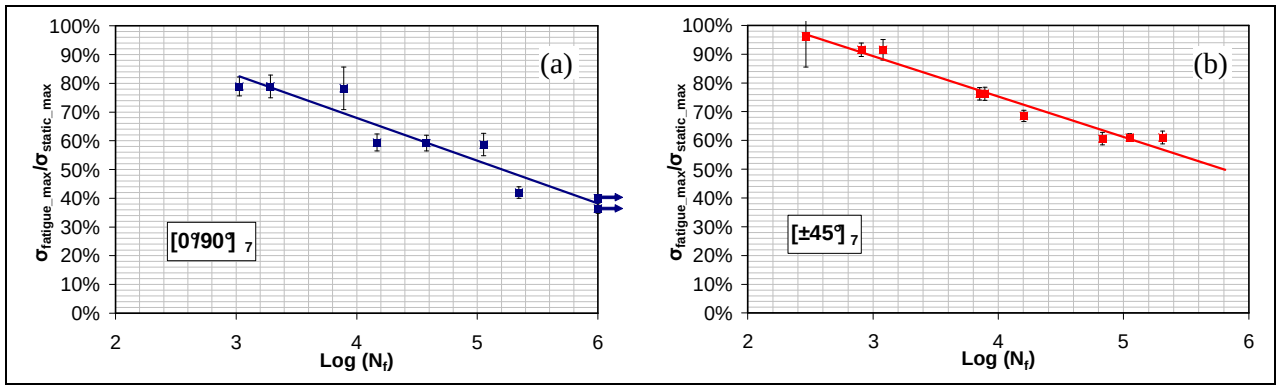


**Figure 5.** Fatigue lifetime results and S-N curves for $[0°/90°]_7$ and $[\pm45°]_7$ hemp/epoxy composites.

*3.2 Damage analysis*

During fatigue tests, three mechanical parameters have been determined at each cycle: the residual secant modulus (slope of the stress-strain curve at the end of the fatigue cycle), the maximal and the residual engineering strain for the considered cycle. The evolution of these mechanical parameters during fatigue test is an indicator of the sample damage evolution. Figures 6, 7 and 8 present these parameters versus the normalized number of cycles ($N/N_f$). Each type of laminate and each level of fatigue stress are plotted in different colors. The presented values are the mean values of measurements obtained during the three repetitions of each type of test. Figure 6 shows the evolution of the residual secant modulus, normalized by the secant modulus of the first cycle of the smallest applied fatigue stress for each laminate (40% $\sigma_{static\_max}$ for the $[0°/90°]_7$ and 60% $\sigma_{static\_max}$ for the $[\pm45°]_7$).

For the $[0°/90°]_7$ laminate, the residual secant modulus decreases to around 80% at final rupture and this decrease is more significant for higher fatigue stress levels (figure 6.a). Curves in figure 6.a have three distinct phases: at the beginning, the modulus evolution starts with a marked decrease, then, during the main part of the test, it has a less accentuated slope, and finally the secant modulus decreases suddenly just before failure. The maximum and minimum strains evolution for this laminate show a strong influence of the applied fatigue stress (figures 7.a and 8.a). Strain evolution curves are also constituted of three phases, keeping an almost constant value during the main part of the fatigue test. Thus, these results show that for these three mechanical parameters, the applied fatigue stress plays a more significant role than the number of fatigue cycles.

For the $[\pm45°]_7$ laminate, results show that, for the three mechanical parameters, there is a more significant influence of the number of fatigue cycles than for the other type of laminate: parameter values change all along the fatigue tests. For the normalized secant modulus, the three curves converge to the same value. We note that the samples loaded to 60% and 75% of static failure stress show similar modulus evolution, with a convergence to the same value at the middle of the fatigue lifetime (figure 6.b). The evolution of maximum and minimum strains is significantly influenced by the applied fatigue stress and also by the fatigue cycle

number (figures 7.b and 8.b). We see no convergence in these parameters evolutions, and the three phases of the curve slopes can also be distinguished.

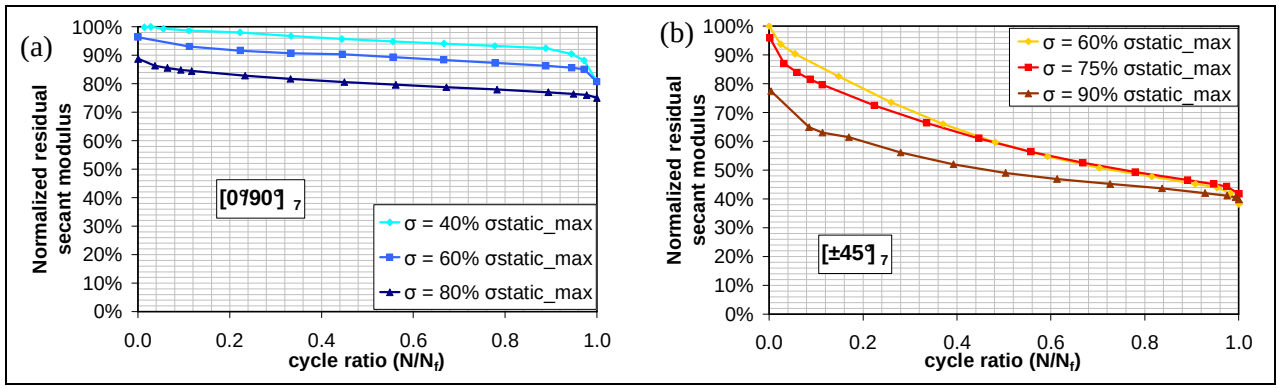


**Figure 6.** Normalized residual secant modulus versus the fatigue cycle number ratio $N/N_f$ for hemp/epoxy composite.

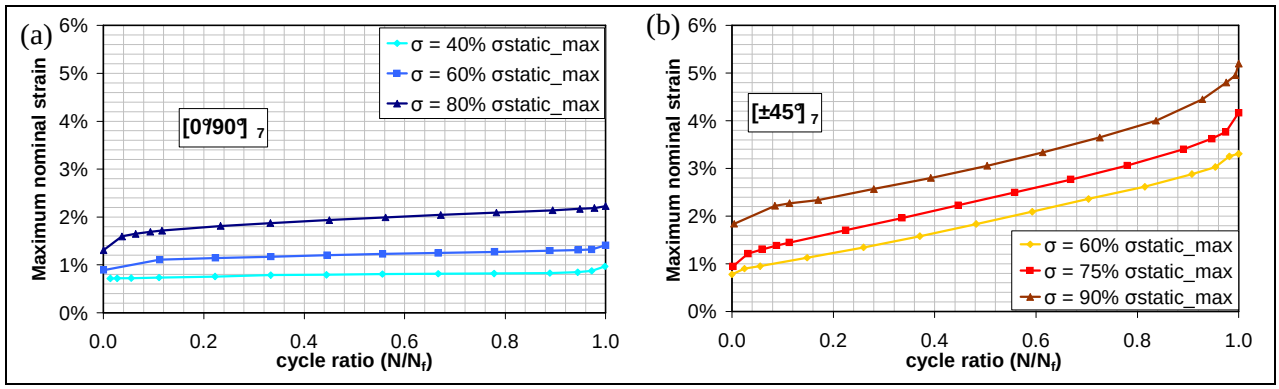


**Figure 7.** Strain at maximum stress for each fatigue cycle for hemp/epoxy composite.

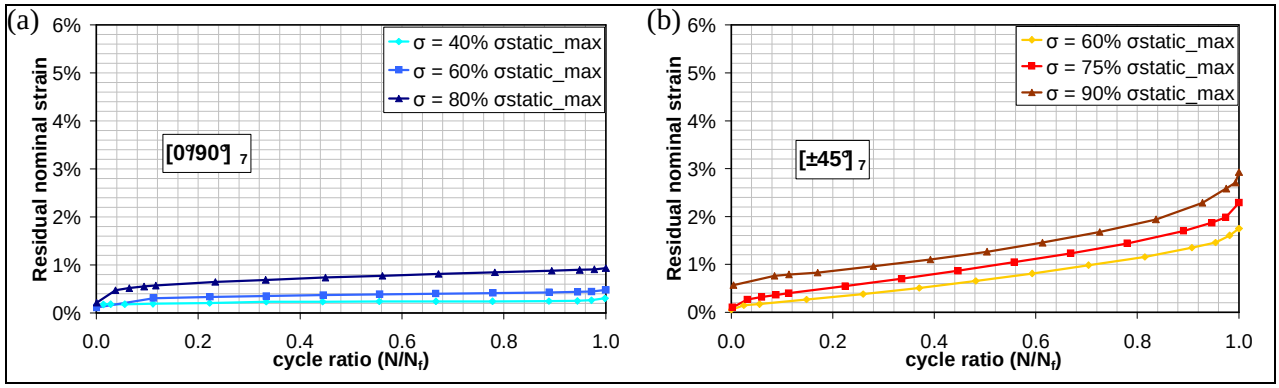


**Figure 8.** Strain at minimum stress for each fatigue cycle for hemp/epoxy composite.

Results of acoustic emission (AE) are shown in the figure 9. Each acoustic event can be associated to damage development [1]. At first, it is obvious that, for the two types of specimens, the total number of acoustic events is directly linked with the fatigue stress level. And this total number is higher in $[\pm 45°]_7$ specimens than in $[0°/90°]_7$ ones: thus, it seems that damage is more significant in the $[\pm 45°]_7$ laminates.

Figure 9 also shows that acoustic events are distributed all along the specimen and throughout the fatigue life, regardless the fatigue stress amplitude, and with a tendency to localize around the failure zone (represented by black diamonds) only at the end of the test. There is a predominance of low amplitudes (35 to 49 dB), whatever the applied fatigue stress, as shown in table 1: there is no significant difference on mean acoustic event amplitude and its standard

deviation for both laminates and for all the fatigue stress levels. But if we look at the average number of acoustic events during each fatigue cycle (figure 10), the strong influence of the applied fatigue stress is shown again.

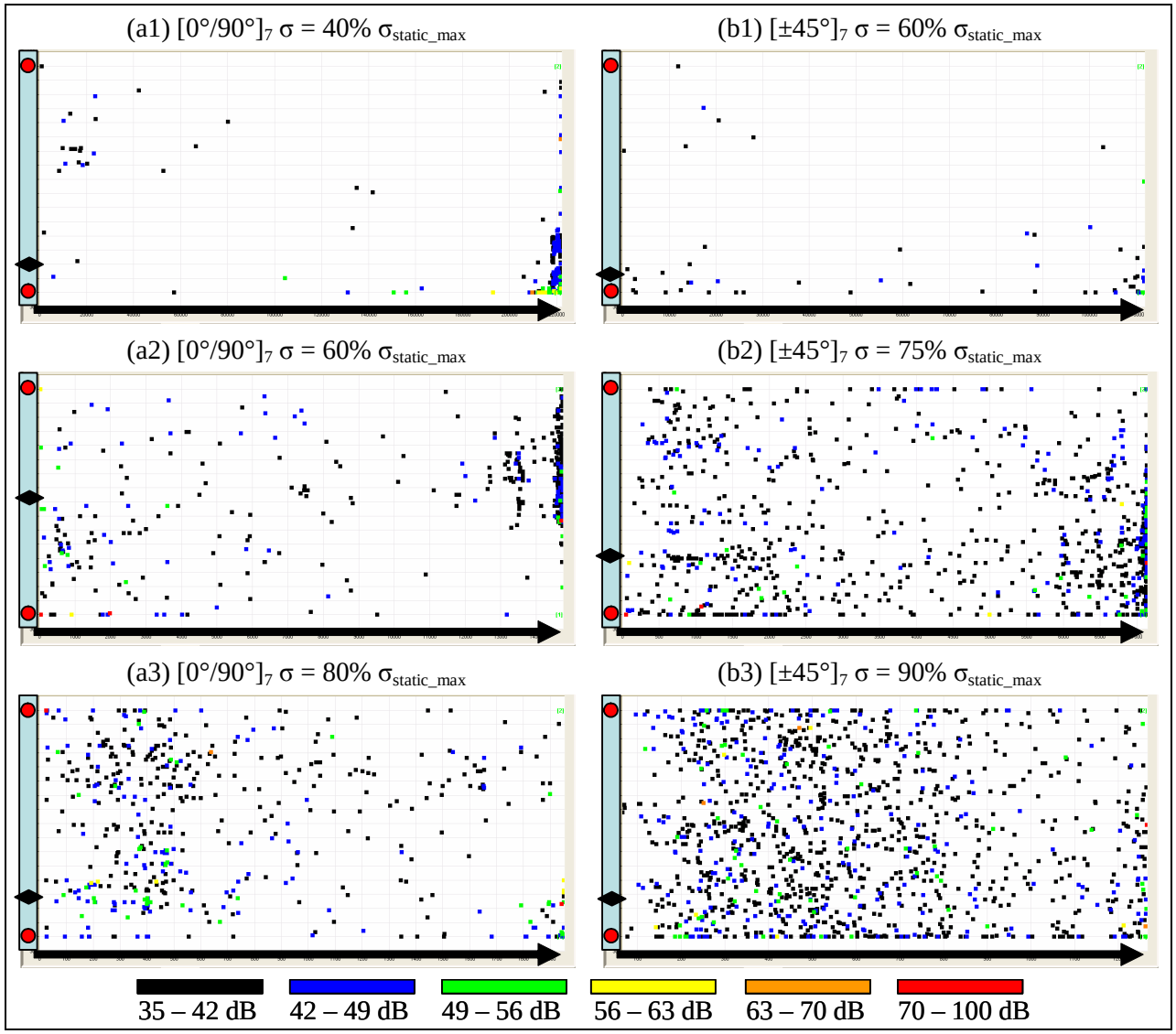


**Figure 9.** Acoustic events recorded on hemp/epoxy composite during fatigue lifetime (horizontal axis), and their location in the specimen (blue rectangle), between the AE captors (red points). Failure zones are represented by black diamonds in the specimens. At the bottom, the color code for amplitude range of acoustic events.

| Specimen | $\sigma_{fatigue\_max}/\sigma_{static\_max}$ | Mean amplitude [dB] | Standard deviation [dB] |
|---|---|---|---|
| $[0°/90°]_7$ | 40 % | 43 | 3 |
| | 60 % | 40 | 6 |
| | 80 % | 41 | 6 |
| $[\pm45°]_7$ | 60 % | 40 | 5 |
| | 75 % | 40 | 5 |
| | 90 % | 40 | 5 |

**Table 1.** Mean amplitude and its standard deviation of acoustic events recorded during fatigue tests on hemp/epoxy composite.

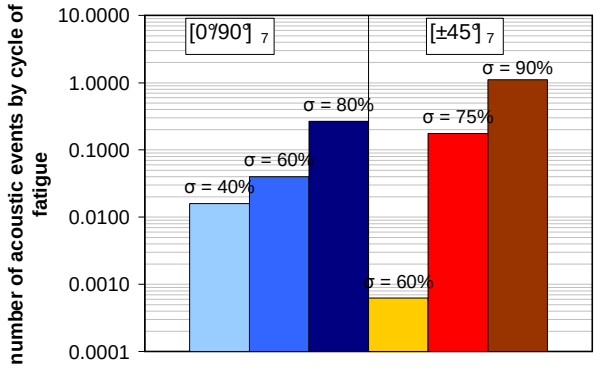


**Figure 10.** Average number of acoustic events by cycle of fatigue recorded on hemp/epoxy samples.

In order to determine more precisely when damage occurs during fatigue testing, we present in figure 11 the acoustic events throughout fatigue life: each event is plotted against the applied stress value at the moment of occurrence of the event (vertical axis). This vertical axis represents the stress value during each fatigue cycle: it starts from around zero, raises to the maximum fatigue stress value and then returns to the minimum stress value. Figure 11 corresponds to fatigue tests with the highest applied stress for $[0°/90°]_7$ and $[\pm45°]_7$ laminates. It shows that the acoustic events are concentrated around the maximum stress value of each cycle, mostly in the upward region (below the red line). These results demonstrate that, during each cycle of fatigue tests on hemp/epoxy laminates, damage preferentially occurs above a stress threshold value, up to the maximum stress value. Few acoustic events occur after the maximum stress value, at the beginning of the unloading. And there is no acoustic event near the minimum stress value. Thus, there are very few events related to crack closure.

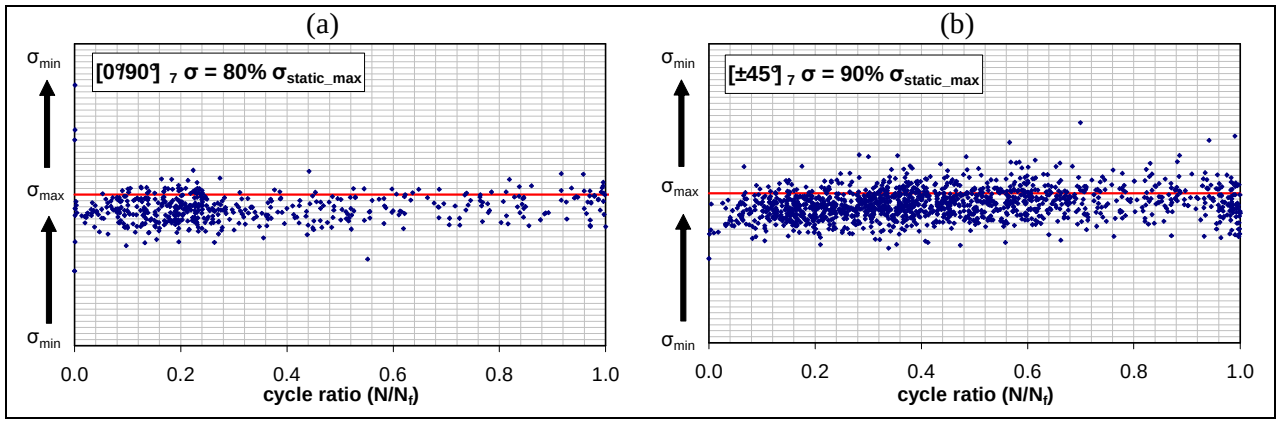


**Figure 11.** Acoustic events throughout fatigue life (horizontal axis), plotted against the applied stress at the moment of occurrence of the event (vertical axis) recorded during fatigue tests on hemp/epoxy laminates.

In the microtomography observations, as presented in figure 12 for both types of laminates after fatigue test, the white zones are hemp yarns, the grey ones are the epoxy matrix and the black ones are empty zones. These observations show that fatigue tests have created matrix cracks at the interface between yarn and matrix that tend to be perpendicular to tensile axis and tend to follow the interface, changing in direction at yarn intersections. These matrix cracks at the interface are distributed throughout the region of each specimen (20x20 $mm^2$ near the rupture) and are found for every fatigue stress level. The empty spheres in the matrix of $[0°/90°]_7$ laminates are porosities that might appear during the manufacturing process.
These matrix cracks could explain the appearance of heat concentration at the rupture zone just before failure, as seen in figure 13 for a $[0°/90°]_7$ laminate. Indeed, the friction of crack surfaces can increase the material temperature. A concentrated heat means a concentration of

cracks and thus a weakened zone, where the occurrence of the final specimen failure is more likely to happen.

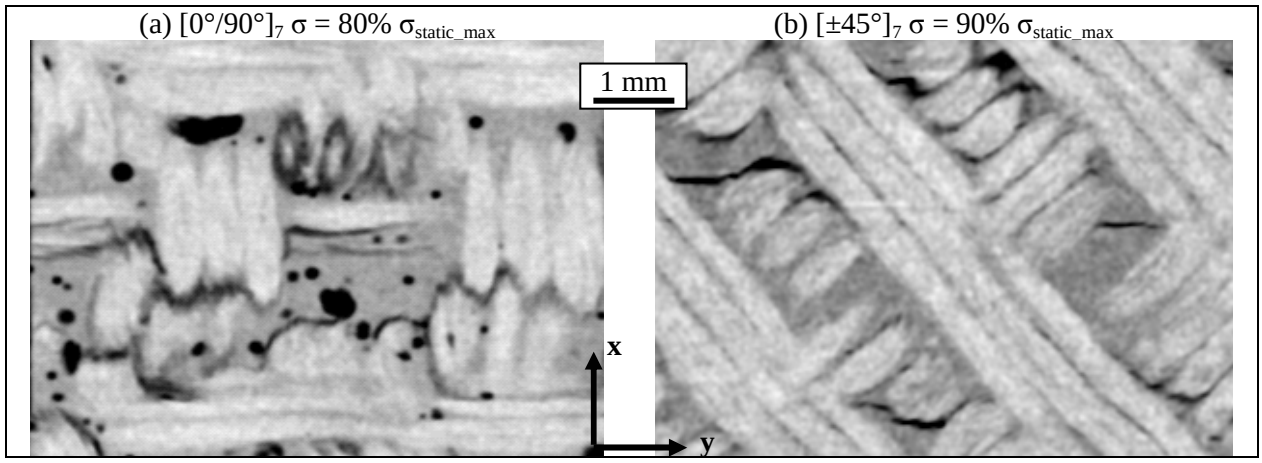


**Figure 12.** X-ray microtomography observations on $[0°/90°]_7$ and $[\pm45°]_7$ hemp/epoxy specimens after fatigue test at 80% and 90% of $\sigma_{static\_max}$, respectively.

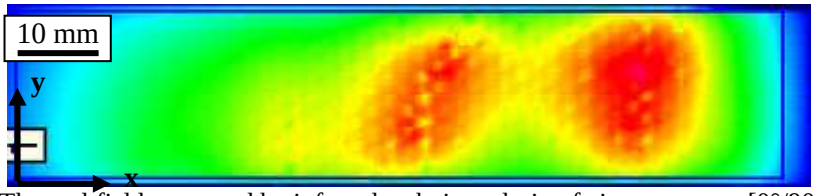


**Figure 13.** Thermal field measured by infrared technique during fatigue test on a $[0°/90°]_7$ hemp/epoxy laminate's front face.

## 4 Conclusions

The cyclic fatigue behavior of a woven hemp/epoxy composite has been studied for two types of laminates: $[0°/90°]_7$ and $[\pm45°]_7$. For each laminate, the Wöhler law has been determined. Significant dispersion due to the natural dispersion of mechanical properties of hemp yarns has been highlighted. The secant modulus during fatigue life shows a significant loss, indicating the creation of damage. AE measurements show, for every laminate and every fatigue stress level, that acoustic events are distributed throughout the specimen gauge and the fatigue life. There is a predominance of low amplitude events (35 to 49 dB) which corresponds to matrix cracks development. Location and distribution of these matrix cracks have been analyzed through X-ray microtomography observations. This damage, leading to internal frictions, is probably the cause of heat concentration observed by infrared camera.

## References

[1] Bonnafous C., Touchard F., Chocinski-Arnault L. Damage mechanisms in hemp-fibre woven fabric composites and comparison with glass-fibre composite. *Polymers and Polymer Composites*, **19**, pp. 543-552 (2011).

[2] Liang S., Gning P.B., Guillaumat L. *Fatigue behavior of flax/epoxy composites* in "Proceedings of *JNC 17*", Poitiers, France, (2011).

[3] Towo A.N., Ansell M.P. Fatigue evaluation and dynamic mechanical thermal analysis of sisal fibre–thermosetting resin composites. *Composites Science and Technology*, **68**, pp. 925-932 (2008).

[4] Yuanjian T. Isaac D.H. Impact and fatigue behaviour of hemp fibre composites. *Composites Science and Technology*, **67**, pp. 3300-3307 (2007).